



# Constraining the optical potential in the search for $\eta$ -mesic ${}^4\text{He}$

M. Skurzok<sup>a,\*</sup>, P. Moskal<sup>a</sup>, N.G. Kelkar<sup>b</sup>, S. Hirenzaki<sup>c</sup>, H. Nagahiro<sup>c,d</sup>, N. Ikeno<sup>e</sup>

<sup>a</sup> Institute of Physics, Jagiellonian University, prof. Stanisława Łojasiewicza 11, 30-348 Kraków, Poland

<sup>b</sup> Departamento de Física, Universidad de los Andes, Cra. 1E, 18A–10, Bogotá, Colombia

<sup>c</sup> Department of Physics, Nara Women's University, Nara 630-8506, Japan

<sup>d</sup> Research Center for Nuclear Physics (RCNP), Osaka University, Ibaraki 567-0047, Japan

<sup>e</sup> Department of Life and Environmental Agricultural Sciences, Tottori University, Tottori 680-8551, Japan

## ARTICLE INFO

### Article history:

Received 3 December 2017

Received in revised form 17 April 2018

Accepted 21 April 2018

Available online 27 April 2018

Editor: V. Metag

### Keywords:

Mesic nuclei

Optical model

Nuclear potential

## ABSTRACT

A consistent description of the  $dd \rightarrow {}^4\text{He}\eta$  and  $dd \rightarrow ({}^4\text{He}\eta)_{\text{bound}} \rightarrow X$  cross sections was recently proposed with a broad range of real ( $V_0$ ) and imaginary ( $W_0$ ),  $\eta$ - ${}^4\text{He}$  optical potential parameters leading to a good agreement with the  $dd \rightarrow {}^4\text{He}\eta$  data. Here we compare the predictions of the model below the  $\eta$  production threshold, with the WASA-at-COSY excitation functions for the  $dd \rightarrow {}^3\text{He}N\pi$  reactions to put stronger constraints on ( $V_0, W_0$ ). The allowed parameter space (with  $|V_0| < \sim 60$  MeV and  $|W_0| < \sim 7$  MeV estimated at 90% CL) excludes most optical model predictions of  $\eta$ - ${}^4\text{He}$  nuclei except for some loosely bound narrow states.

© 2018 The Author(s). Published by Elsevier B.V. This is an open access article under the CC BY license (<http://creativecommons.org/licenses/by/4.0/>). Funded by SCOAP<sup>3</sup>.

## 1. Introduction

Mesic nuclei are currently one of the hottest topics in nuclear and hadronic physics, both from experimental [1–5] and theoretical points of view [6–25]. This exotic nuclear matter is supposed to consist of a nucleus bound via the strong interaction with a neutral meson such as the  $\eta$ ,  $\eta'$ ,  $K$  or  $\omega$ . Although, its existence has been predicted over thirty years ago, it still remains to be one of the undiscovered nuclear objects. Some of the most promising candidates for such bound states are  $\eta$ -mesic nuclei, postulated by Haider and Liu in 1986 [26] following the coupled channel calculations by Bhalerao and Liu [27] which reported an attractive  $\eta$ -nucleon interaction. Current studies of hadron- and photon-induced production of the  $\eta$  meson resulting in a wide range of values of the  $\eta N$  scattering length,  $a_{\eta N}$ , indicate the interaction between the  $\eta$  meson and a nucleon to be attractive and strong enough to create an  $\eta$ -nucleus bound system even in light nuclei [7–10,28–30]. However, experiments performed so far have not brought a clear evidence of their existence [31–38]. They provide only signals which might be interpreted as indications of the  $\eta$ -mesic nuclei. The interested reader can find recent reviews on the  $\eta$  mesic bound states searches in Refs. [4,5,14,16,39–44].

Some of the promising experiments related to  $\eta$ -mesic nuclei have been performed with the COSY facility [45]. The most re-

cent of these involves the measurement of the  $dd \rightarrow {}^3\text{He}n\pi^0$  and  $dd \rightarrow {}^3\text{He}p\pi^-$  reactions which has been performed by the WASA-at-COSY Collaboration. Due to the lack of theoretical predictions for cross sections below the  $\eta$  production threshold, the data have been analyzed assuming that the signal from the bound state has a Breit–Wigner shape [1,2]. However, a better guidance for the shape of the cross sections for the  $dd \rightarrow ({}^4\text{He}-\eta)_{\text{bound}} \rightarrow {}^3\text{He}N\pi$  processes is provided by a theoretical model described in Ref. [6] in the excess energy range relevant to the  $\eta$ -mesic nuclear search. Given that the model is the very first attempt to provide a consistent description of the data below and above the  $\eta$  meson production threshold, the authors used a phenomenological approach with an optical potential for the  $\eta$ - ${}^4\text{He}$  interaction. The available data on the  $dd \rightarrow {}^4\text{He}\eta$  reaction is reproduced quite well for a broad range of optical potential parameters for which the authors predict the cross section spectra corresponding to  $\eta$ - ${}^4\text{He}$  bound state formation in the subthreshold region. In this article we present a comparison between this new theoretical model and experimental data collected by WASA-at-COSY in order to further constrain the range of the allowed  $\eta$ - ${}^4\text{He}$  optical potential parameters. The latter, as we shall see, narrows down the search for  $\eta$ -mesic helium to a region of small binding energies and widths.

## 2. Theoretical model

The formalism presented in Ref. [6] predicted for the first time, the formation rate of the  $\eta$ -mesic  ${}^4\text{He}$  in the deuteron–deuteron

\* Corresponding author.

E-mail address: [magdalena.skurzok@uj.edu.pl](mailto:magdalena.skurzok@uj.edu.pl) (M. Skurzok).

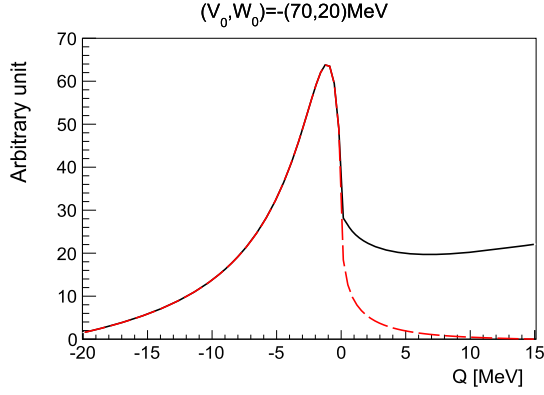


**Fig. 1.** Calculated total cross section of the  $dd \rightarrow (^4\text{He}-\eta)_{\text{bound}} \rightarrow ^3\text{He}N\pi$  reaction for the formation of the  $^4\text{He}-\eta$  bound system plotted as function of the excess energy  $Q$  for  $\eta$ - $^4\text{He}$  optical potential parameters  $(V_0, W_0) = -(70, 20)$  MeV. The black solid line denotes the total cross section  $\sigma$ , while the red dashed line denotes the conversion part  $\sigma_{\text{conv}}$ . (For interpretation of the colors in the figure(s), the reader is referred to the web version of this article.)

fusion reaction within a model which reproduced the data on the  $dd \rightarrow ^4\text{He}\eta$  reaction quite well. The authors determined the total cross sections for the  $dd \rightarrow (^4\text{He}-\eta)_{\text{bound}} \rightarrow ^3\text{He}N\pi$  reaction based on phenomenological calculations. The calculated total cross section  $\sigma$  consists of two parts: conversion  $\sigma_{\text{conv}}$  and escape  $\sigma_{\text{esc}}$  part. The conversion part, determined for different parameters  $V_0$  and  $W_0$  of a spherical  $\eta$ - $^4\text{He}$  optical potential  $V(r) = (V_0 + iW_0) \frac{\rho_\alpha(r)}{\rho_\alpha(0)}$ , is equal to the total cross section in the subthreshold excess energy region where the  $\eta$  meson is absorbed by the nucleus (its energy is not enough to escape from the nucleus), while the  $\eta$  meson escape part contributes to the excess energy region above the threshold for  $\eta$  production and can be calculated as  $\sigma_{\text{esc}} = \sigma - \sigma_{\text{conv}}$ . Fig. 1 shows the example of a calculated total cross section for  $\eta$ - $^4\text{He}$  optical potential parameters  $(V_0, W_0) = -(70, 20)$  MeV.

We should mention here that the above theoretical calculations (which are being used in the present work) were done assuming the one-nucleon absorption of the  $\eta$  meson since the strength of the multi-nucleon absorption processes is not well known. Based on the experimental data on the  $pn \rightarrow d\eta$  and  $pN \rightarrow pN\eta$  reactions, the strength of the  $\eta$  meson absorption by a two-nucleon pair at the nuclear center was estimated in [46] to be 4.2 MeV and 0.2 MeV for the spin triplet and singlet nucleon pairs, respectively. This strength can be larger for  $^4\text{He}$  because of the higher central density as mentioned in [47]. The values of the  $W_0$  parameters in the present work could be compared with these numbers to get a rough estimate of the ratio of the one- and two-body absorption probability at the nuclear center. The two body absorption potential is expected to provide an additional contribution to the conversion cross section. However, it is only the one-nucleon absorption cross section which should be compared with the present data since multi-nucleon absorption processes would contribute to different final states not considered in the present work. Thus, the present analysis of experimental data from Ref. [1] based on the theoretical calculation assuming the one-body absorption seems reasonable.

The spectrum has been normalized in the sense that the escape part reproduces the measured cross sections for the  $dd \rightarrow ^4\text{He}\eta$  process [48–50]. Moreover, the flat contribution in the conversion spectrum, considered to be a part of the background, has been subtracted (taking the minimum value of the  $\sigma_{\text{conv}}$  in the excess energy range from  $-20$  to  $15$  MeV).

Since the signal from the  $\eta$ -mesic bound system is expected below the threshold for the  $\eta$  meson production, the authors focused

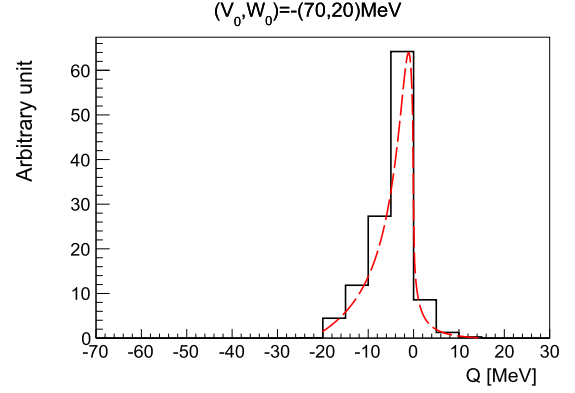


**Fig. 2.** Calculated conversion part of the cross section of the  $dd \rightarrow (^4\text{He}-\eta)_{\text{bound}} \rightarrow ^3\text{He}N\pi$  reaction for the formation of the  $^4\text{He}-\eta$  bound system plotted as a function of the excess energy  $Q$  for  $\eta$ - $^4\text{He}$  optical potential parameters  $(V_0, W_0) = -(70, 20)$  MeV. The cross section is scaled by fitting the escape part to the existing  $dd \rightarrow ^4\text{He}\eta$  data and the flat contribution is subtracted as well. The red dashed line shows the theoretical spectrum while the black solid line shows the spectrum after binning (details in Sec. 3).

here only on the conversion part of the cross sections. An example of the calculated  $\sigma_{\text{conv}}$  is shown in Fig. 2 for potential parameters  $(V_0, W_0) = -(70, 20)$  MeV. The authors of Reference [6] concluded that as a next step it would be important to compare these theoretical results with the experimental data, convoluting the theoretical cross sections with the experimental resolution functions. In this article we present results of such a comparison. The details are presented in Section 4 which will be preceded by a brief description of the experimental conditions.

### 3. Experimental data

Recent measurements at WASA-at-COSY, dedicated to search for  $\eta$ -mesic  $^4\text{He}$  nuclei were carried out using the unique ramped beam technique allowing for the beam momentum to be changed slowly and continuously around the  $\eta$  production threshold in each of the acceleration cycles [1,2,42,44]. This technique allows to reduce systematic uncertainties with respect to separate runs at fixed beam energies [2,34,51]. The  $^4\text{He}-\eta$  bound states were searched by studying the excitation functions for  $dd \rightarrow ^3\text{He}n\pi^0$  and  $dd \rightarrow ^3\text{He}p\pi^-$  processes in the excess energy range  $Q$  from  $-70$  MeV to  $30$  MeV. The obtained excitation functions do not reveal any direct narrow structure below the  $\eta$  production threshold, which could be considered as a signature of the bound state. Therefore, only the upper limit of the total cross section for the  $\eta$ -mesic  $^4\text{He}$  formation was determined.

In the first approach, the upper limits of the total cross sections for both processes were estimated at a 90% confidence level (CL) fitting simultaneously the excitation functions with a sum of a Breit-Wigner and a second order polynomial function corresponding to the bound state signal and background, respectively. Moreover, the isospin relation between  $n\pi^0$  and  $p\pi^-$  pairs was taken into account. The corresponding data analysis is presented in detail in Ref. [1]. The analysis resulted in the value of the upper limit in the range from  $2.5$  to  $3.5$  nb for the  $dd \rightarrow (^4\text{He}-\eta)_{\text{bound}} \rightarrow ^3\text{He}n\pi^0$  process and from  $5$  to  $7$  nb for the  $dd \rightarrow (^4\text{He}-\eta)_{\text{bound}} \rightarrow ^3\text{He}p\pi^-$  reaction. Systematic uncertainty, contributed mainly from the assumption of the Fermi momentum of the  $N^*$  resonance inside  $^4\text{He}$  [13], to be equal to that of a nucleon in  $^4\text{He}$  [52], varies from  $42\%$  to  $46\%$  for both reactions.

These experimental results are revisited in the next section in the light of a new theoretical model [6] which reproduces the  $dd \rightarrow ^4\text{He}\eta$  cross section data and with the same  $\eta$ - $^4\text{He}$  optical

potential predicts the cross sections for  $dd$  fusion with the formation of an  $\eta$ -mesic  ${}^4\text{He}$  below the  $\eta$  production threshold. The objective of the present analysis is twofold: (i) to provide stronger constraints on the optical potential parameters which are already capable of reproducing the  $\eta$  production data and (ii) to improve the upper limits on the cross sections found in [1] using a theoretical model (constrained by the above threshold data) for the possible bound state, rather than the simple Breit-Wigner form used in [1].

#### 4. Comparison between theory and data: results and discussion

As mentioned in the previous section, we performed the analysis which allows to compare excitation functions measured for  $dd \rightarrow {}^3\text{He}n\pi^0$  and  $dd \rightarrow {}^3\text{He}p\pi^-$  processes [1] with the theoretical predictions presented in Ref. [6]. For this purpose, theoretical conversion spectra were convoluted with the experimental resolutions of the excess energy  $Q$ . The COSY beam is characterized by a high momentum resolution of up to  $\frac{\Delta p}{p} \approx 1 \cdot 10^{-4}$  resulting in the resolution of  $\Delta Q$  of about 70 keV in the energy range of interest. This is about 70 times smaller than the binning of the spectra used by the WASA-at-COSY collaboration [1]. Hence, we bin the theoretical predictions in the same way as data, dividing the spectra into 20 intervals each of 5 MeV width. We assume also that the reconstruction efficiency in the WASA-at-COSY experiment is in a good approximation independent of the excess energy  $Q$  as was proven in Ref. [53]. An example of the theoretical spectrum after the binning procedure is presented in Fig. 2 as a black histogram.

In the next step, the experimental excitation functions for  $dd \rightarrow {}^3\text{He}n\pi^0$  and  $dd \rightarrow {}^3\text{He}p\pi^-$  reactions were fitted simultaneously with a sum of binned theoretical function (signal) and a second order polynomial (background). The  $n\pi^0$ ,  $p\pi^-$  isospin relation was taken into account. The fitting functions can be presented as follows:

$$\sigma_{n\pi^0}(Q) = \frac{1}{3}A \cdot \text{Theory}(Q) + B_1 Q^2 + C_1 Q + D_1 \quad (1)$$

$$\sigma_{p\pi^-}(Q) = \frac{2}{3}A \cdot \text{Theory}(Q) + B_2 Q^2 + C_2 Q + D_2 \quad (2)$$

for  $dd \rightarrow {}^3\text{He}n\pi^0$  and  $dd \rightarrow {}^3\text{He}p\pi^-$ , respectively.  $\text{Theory}(Q)$  denotes the theoretical function after binning with the amplitude normalized to unity, while  $B_{1,2}Q^2 + C_{1,2}Q + D_{1,2}$  is a polynomial of the second order. The fit was performed for theoretical spectra obtained for different optical potential parameters ( $V_0, W_0$ ) [6]. During the fit, the amplitude  $A$  of the theoretical spectrum and polynomial coefficients were treated as free parameters. As an example, the excitation functions with the fit results for optical potential parameters ( $V_0, W_0$ ) =  $-(70, 20)$  MeV are presented in Fig. 3.

The performed fit delivers the amplitudes  $A$  for  $dd \rightarrow {}^3\text{He}n\pi$  consistent with zero within  $2\sigma$  for all sets of  $V_0, W_0$  parameters, which is given in Table 1.

Therefore, the upper limit of the total cross section was determined, like in Ref. [1], at the confidence level 90% based on standard deviation of the amplitude  $\sigma_A$  ( $\sigma_{A}^{CL=90\%} = 1.64 \cdot \sigma_A$ ).  $\sigma_{upp}^{CL=90\%}$  values are presented for different parameters  $V_0, W_0$  in Table 1.

Obtained  $\sigma_{upp}^{CL=90\%}$  is weakly sensitive to the  $V_0, W_0$  parameters, varying from 5.2 to 7.4 nb. Taking into account the systematic uncertainties of about 44% estimated in Ref. [1], the values increase, varying from about 7.5 to 10.7 nb. Therefore, in the contour plot shown in Fig. 4, we exclude the region where the cross section is above 10.7 nb (light shaded area). Dark shaded area shows the systematic error. The latter estimate is based on a calculation [13] for the  $N^*$  momentum distribution for a given set of  $\pi NN^*$  and

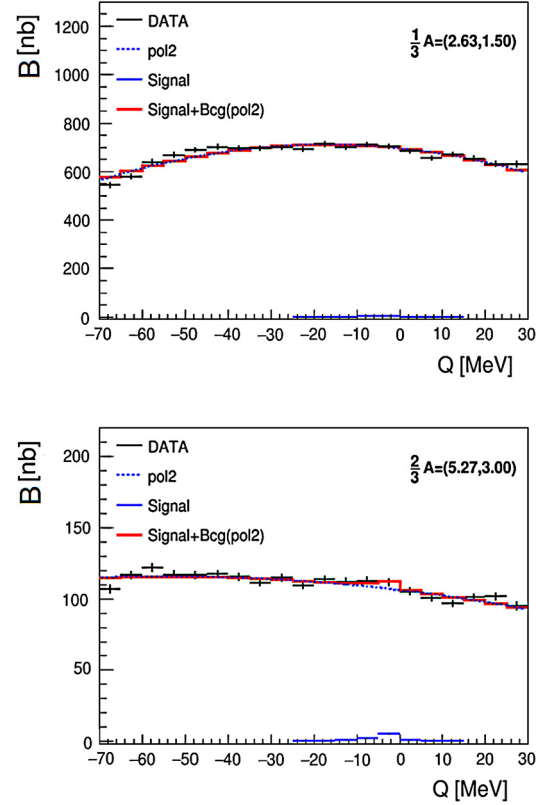


**Fig. 3.** Excitation function of variable  $B = \frac{N}{L_e}$  for  $dd \rightarrow {}^3\text{He}n\pi^0$  (upper panel) and  $dd \rightarrow {}^3\text{He}p\pi^-$  reaction (lower panel) determined as described in Ref. [1]. The red solid line represents a fit with theoretical prediction for potential parameters ( $V_0, W_0$ ) =  $-(70, 20)$  MeV combined with a second order polynomial. The blue dotted line shows the second order polynomial describing the background while the blue solid line shows the signal contribution. The experimental data [1] are indicated with black line.

**Table 1**

Results obtained from the fit of theoretical spectra to experimental data. Table includes: optical potential parameters (first and second columns), amplitude obtained from the fit with its statistical uncertainty (third column) and upper limit of the total cross section for the  $dd \rightarrow ({}^4\text{He}-\eta)_{\text{bound}} \rightarrow {}^3\text{He}n\pi$  process at CL = 90% (fourth column).

$V_0$	$W_0$	$A$ (fit) [nb]	$\sigma_{upp}^{CL=90\%}$ [nb]
-30	-5	$-5.0 \pm 3.9$	6.5
-30	-20	$-2.2 \pm 3.5$	5.8
-30	-40	$0.2 \pm 3.8$	6.3
-50	-5	$0.1 \pm 3.8$	6.3
-50	-20	$3.3 \pm 4.1$	6.8
-50	-40	$6.0 \pm 4.2$	6.9
-70	-5	$6.4 \pm 4.5$	7.4
-70	-20	$7.9 \pm 4.5$	7.4
-70	-40	$7.5 \pm 3.7$	6.1
-100	-5	$6.3 \pm 4.5$	7.4
-100	-20	$6.9 \pm 3.9$	6.4
-100	-40	$5.3 \pm 3.1$	5.2

$\eta NN^*$  coupling constants. If we take into account the calculations in [13] using all available values of the coupling constants, the allowed region in the  $V_0$ - $W_0$  plane can extend as far as the red line shown in Fig. 4. The colored dots shown in the figure are the results of some optical model calculations which will be discussed in the next section.

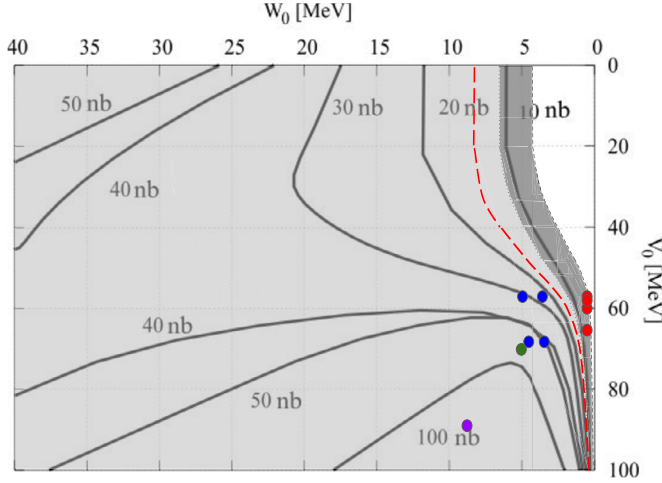


**Fig. 4.** Contour plot of the theoretically determined conversion cross section in  $V_0$ - $W_0$  plane [6]. Light shaded area shows the region excluded by our analysis, while the dark shaded area denotes systematic uncertainty of the  $\sigma_{\text{upper}}^{CL=90\%}$ . The red line extends the allowed region based on a new estimate of errors (see text for details). Dots correspond to the optical potential parameters corresponding to the predicted  $\eta$ -mesic  ${}^4\text{He}$  states.

### 5. Optical model predictions of $\eta$ -mesic ${}^4\text{He}$

After constraining the region of the optical potential ( $V_0$ ,  $W_0$ ) parameter space allowed by the cross section data below the  $\eta$  production threshold, let us now examine the possibility for the existence of  $\eta$ -mesic helium nuclei predicted within the optical model. To start with, we notice that all states predicted in Table 1 of [6] by solving the Klein Gordon equation with the optical potential of the present work, are excluded. On the other hand, since a wide range of  $V_0$ ,  $W_0$  values in [6] do reproduce the  $dd \rightarrow \eta$  data, it seems worthwhile to investigate other optical model predictions in the literature.

The authors in [10] for example, compare their results using a few body formalism with existing optical model calculations by using the following form of the  $\eta$ - ${}^4\text{He}$  potential with the complex  $\eta$ -nucleon scattering amplitude  $F_{\eta N}$  chosen from two different models in literature [54,55]:

$$V(r) = -\frac{6\pi}{\mu_{\eta N}} F_{\eta N} (r_0\sqrt{\pi})^{-3} \exp(-\frac{r^2}{r_0^2}). \quad (3)$$

Replacing the parameter,  $r_0 = 1.267$  fm, as given in [10] and rewriting the above equation for the potential as,  $V(r) = [V_0 + iW_0] \exp(-r^2/r_0^2)$ , we identify the strengths  $V_0$  and  $W_0$  and list them in Table 2 for the different cases listed in Table 4 of Ref. [10]. The  $\eta N$  amplitude of [54] (GW), was obtained within a K-matrix description of the  $\pi N$ ,  $\pi\pi N$ ,  $\eta N$  and  $\gamma N$  coupled channels. The authors fitted the  $\pi N \rightarrow \pi N$ ,  $\pi N \rightarrow \eta N$ ,  $\gamma N \rightarrow \pi N$  and  $\gamma N \rightarrow \eta N$  data in the energy range of about 100 MeV on either side of the  $\eta$  threshold. Ref. [55] presented the  $\eta N$  amplitudes calculated within a chirally motivated separable potential model with the parameters of the model fitted to  $\pi N \rightarrow \pi N$  and  $\pi N \rightarrow \eta N$  data. A comparison of the  $V_0$  and  $W_0$  values in Table 2 with the allowed region of the  $V_0$ - $W_0$  plane leads us to the conclusion that all the bound states listed in Table 2 are excluded by our analysis.

Having excluded the optical potential predictions of unstable bound states in literature, we turn to examine the special case of an unstable state centered at zero energy. The case of a zero energy bound state (or zero energy resonance), sometimes referred to as a transition state [56] has been widely studied in literature [57] in the context of different physical situations and has

also been observed in ultracold atoms [58]. Let us recall some basic facts: a bound state corresponds to a pole in the S-matrix for  $E < 0$ . A resonance corresponds to a pole at positive energies. A state at  $E = 0$  (which is usually referred to as a zero energy bound state in case the angular momentum  $l > 0$  and zero energy resonance otherwise) leads to a scattering length,  $a \rightarrow \infty$ , i.e., the scattering amplitude has a pole when  $E = 0$ . Ref. [56] has examined the occurrence of such states for a class of potentials of the form  $V(r, r_0) = -\frac{g}{r^s} f\left(\frac{r}{r_0}\right)$  ( $g > 0$ ,  $r_0 > 0$ ), which include the Gaussian, exponential and Hulthen among others. For the Gaussian optical potential of the present work, we identify  $g$  with  $V_0$ ,  $s = 0$  and  $f = \exp(-r^2/r_0^2)$ . Analytical as well as numerical solutions of the Schroedinger equation for these potentials are provided in Ref. [56]. It is shown that the existence of the transition state solution depends on a critical parameter given by  $\beta = 2\mu V_0 r_0^2/\hbar^2$ , numerical values of which are listed in a table for several values of  $l$ . Taking their value of  $\beta = 2.684$  in case of the Gaussian potential with  $l = 0$ ,  $\mu$  the reduced mass of  $\eta$ - ${}^4\text{He}$  and with  $r_0 = 1.267$  fm, we find  $V_0 = -68.04$  MeV. Putting back this value in the expression,  $V_0 = -[6\pi/\mu_{\eta N}] \Re F_{\eta N} (r_0\sqrt{\pi})^{-3}$ , arising from (3), we determine  $\Re F_{\eta N} = 0.364$  fm. This value of  $\Re F_{\eta N}$  corresponds to the subthreshold energies of  $\sqrt{s} = 1418.2$  and 1467 MeV of the GW and CS  $\eta N$  amplitudes respectively (see Fig. 1 in Ref. [10]). The imaginary parts of the amplitudes can be seen from the same figure in [10] (at the corresponding energies) to be  $\Im F_{\eta N} = 0.0167$  fm and  $\Im F_{\eta N} = 0.0245$  fm for the GW and CS models respectively. The imaginary part of the optical potential can now be determined using,  $W_0 = -[6\pi/\mu_{\eta N}] \Im F_{\eta N} (r_0\sqrt{\pi})^{-3}$ .

Thus, in case of the zero energy resonance, we find the optical potential parameters, ( $V_0$ ,  $W_0$ ) to be  $(-68.04, -3.12)$  MeV and  $(-68.04, -4.55)$  MeV for the GW and CS  $\eta$ -nucleon interactions respectively. Repeating the exercise for a different value of the Gaussian parameter,  $r_0 = 1.373$  fm as in [6], the potential parameters are found to be  $(-58.01, -3.2)$  MeV and  $(-58.01, -4.9)$  MeV for the GW and CS  $\eta$ -nucleon interactions respectively.

The above method of first considering the  $E = 0$  state of a real Gaussian potential to determine  $V_0$  and then finding  $W_0$  seems a posteriori justified considering the small values of  $W_0$  (as compared to  $V_0$ ) obtained. Indeed a similar procedure of first finding the binding energy by considering only the real part of the potential and later finding  $\Gamma = -2 < \Psi | \Im m V_{\eta A} | \Psi >$  using perturbation theory where  $\Psi$  is the solution of the real Hamiltonian has been used in [10] too.

Finally, motivated by the above discussion, a renewed search for the  $\eta$ - ${}^4\text{He}$  states within the model of [6] is performed. At the edge of the allowed region in Fig. 4, very narrow and weakly bound states of  $\eta$ - ${}^4\text{He}$ , with binding energies and widths in the range of  $\sim 2$ –230 keV and  $\sim 8$ –64 keV respectively are found by solving the Klein Gordon equation as in [6]. These states correspond to the optical potential parameters  $|V_0|$  in the range from 58 to 65 MeV and  $W_0 = 0.5$  MeV (red dots in Fig. 4). For values of  $|V_0| < 58$  MeV, no bound states are found. We should mention here, however, that some of the potential parameters are not consistent with the experimental data on the  $\eta$  production cross section above threshold as reported in Ref. [6], especially for the cases with weak absorption. Hence we think that a systematic analysis including both the escape and the conversion cross sections covering the above- and below-threshold region is necessary in order to investigate the weak absorptive potential region.

### 6. Subthreshold considerations and uncertainties

The  $\eta$ -nucleus optical potentials are in principle energy dependent and would depend strongly for example on the energy



**Table 2**

Strength of the optical potentials corresponding to the  $\eta$ - $^4\text{He}$  states given in [10].  $\delta\sqrt{s} = \sqrt{s} - \sqrt{s_{th}}$  with  $\sqrt{s}$  being the energy available in the center of mass of the  $\eta N$  system.  $B_{\eta^4\text{He}}$  and  $\Gamma$  are the binding energies and widths of the  $\eta$ - $^4\text{He}$  states.

$\eta N$ model	$\delta\sqrt{s}$ [MeV]	$B_{\eta^4\text{He}}$ [MeV]	$\Gamma$ [MeV]	$-V_0$ [MeV]	$-W_0$ [MeV]
GW [54]	0	25.1	40.8	175.7	54.2
	-32.4	1.03	2.35	89.7	8.6
CS [55]	0	6.39	21	125.87	29.35
	-19.2	-	-	69.15	5.046

at which the elementary  $\eta N$  amplitude,  $F_{\eta N}$ , of Eq. (3) is evaluated. In the case of  $\eta$ -mesic nuclei, the  $\eta N$  interaction happens at subthreshold energies and  $F_{\eta N}$  should be evaluated at an energy shifted by an amount  $\delta$  below threshold. The importance of taking such a downward shift into account has been discussed with different points of view in literature [59–62]. The authors in [59,60] (and references therein) provide a detailed analysis of this topic and derive an expression for  $\delta$  which depends on the nuclear binding energy per nucleon as well as the real part of the optical potential itself. Refs. [61,62], however, provide a simpler method with  $\delta$  given by the average binding of the target nucleons.

Since the experimental analysis of the present work relies on the input from the theoretical calculations in [6] where the above effects were not taken into account explicitly, we shall now try to estimate the uncertainties on  $\sigma_{upp}$  (shown by the red mesh in Fig. 5) introduced by this omission. To obtain this estimate, we evaluate the optical potential parameters  $V_0$ ,  $W_0$  using Eq. (3) by comparing them with the form  $V(r) = [V_0 + iW_0]\exp(-\frac{r^2}{r_0^2})$ . Thus, as observed in the previous section,  $V_0 = -[6\pi/\mu_{\eta N}]\Re F_{\eta N}(r_0\sqrt{\pi})^{-3}$  and  $W_0 = -[6\pi/\mu_{\eta N}] \times \Im F_{\eta N}(r_0\sqrt{\pi})^{-3}$ . Evaluating  $F_{\eta N}$  at threshold and at 7 MeV (binding energy per nucleon for  $^4\text{He}$ ) and 30 MeV below threshold, we obtain the optical potential parameters given in Table 2 for different models of  $F_{\eta N}$  [54,55,63–65] in literature. The values of  $\sigma_{upp}$  corresponding to the parameters  $V_0$ ,  $W_0$  in Table 2 are read off from Fig. 5 and listed in Table 3. Even if the optical potential parameters do change a lot depending on the choice of the energy at which  $F_{\eta N}$  is evaluated, the upper limits on the cross sections do not seem to be very sensitive to this change. Depending on the model, the change in the upper limits can be between 0–6%. Given that the upper limits  $\sigma_{upp}$  determined in the present analysis are not very sensitive to the parameters  $V_0$ ,  $W_0$  (see Table 1 and Fig. 5), such a small uncertainty was expected.

## 7. Summary and conclusions

We performed an analysis in order to constrain the  $\eta$ - $^4\text{He}$  optical potential parameters by comparing a recently developed theoretical model for  $\eta$ - $^4\text{He}$  bound state production in  $dd \rightarrow ^3\text{He}N\pi$  reactions [6] with the experimental data collected by WASA-at-COSY [1]. Convoluting the theoretical cross section with experimental resolutions, we estimated the upper limits of the total cross

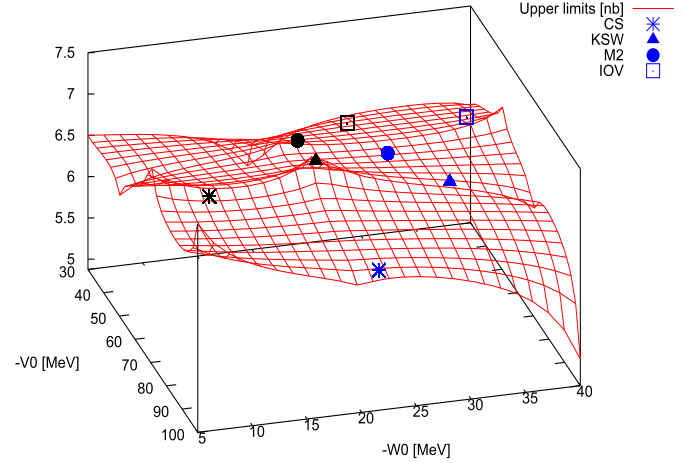


**Fig. 5.** Upper limits on the cross sections,  $\sigma_{upp}$  in nb, as a function of the optical potential parameters  $V_0$  and  $W_0$ . The red mesh represents the values determined in the present analysis (as in Table 1). The symbols are the values of  $\sigma_{upp}$  corresponding to  $V_0$ ,  $W_0$  given in Table 2 for the different  $\eta N$  models. The black symbols correspond to  $\sigma_{upp}$  for  $V_0$ ,  $W_0$  evaluated using  $F_{\eta N}$  at a subthreshold  $\eta N$  centre mass energy of  $\sqrt{s} - 7$  MeV and the blue symbols with  $F_{\eta N}$  at threshold.

sections for the formation of the  $\eta$ -mesic Helium nuclei in  $dd \rightarrow ^3\text{He}N\pi$  processes at a 90% confidence level.

Comparison of the determined upper limits for the creation of  $\eta$ -mesic nuclei via the  $dd \rightarrow ^3\text{He}N\pi$  processes with the cross sections obtained in Ref. [6] excludes a wide range of  $\eta$ - $^4\text{He}$  optical potential parameters. With the values of  $|V_0|$  and  $|W_0|$  being restricted to be less than 60 MeV and 7 MeV respectively, most predictions of  $\eta$ -mesic helium states seem to be excluded within the present analysis. Extremely narrow and loosely bound states within the model of [6] seem however to appear in the allowed region of the optical potential parameters.

In spite of some shortcomings such as the absence of the explicit inclusion of the strong energy dependence of the  $\eta N$  interaction [60] and the fact that, in principle, the  $\eta$ -helium nuclei should be treated within a few body formalism [8,10,66,67], it is worth noting that in the decades long search for  $\eta$ -mesic nuclei, the present work is indeed a first attempt to combine the experimental data below  $\eta$  production threshold with predictions from a theoretical model which can reproduce the existing data above threshold too. There exist approaches such as the coupled channels

**Table 3**

Optical potential parameters  $V_0$  and  $W_0$  (in MeV) evaluated using (3) with the  $\eta$ - $N$  amplitude  $F_{\eta N}$  evaluated at  $\delta = 0$  (threshold),  $\delta = -7$  MeV and  $\delta = -30$  MeV, with  $\delta = \sqrt{s} - \sqrt{s_{th}}$ . The upper limits on the cross sections listed in this table are read from the mesh (representing the  $\sigma_{upp}$  (in nb) determined in the present analysis) in Fig. 5 at the values of  $V_0$  and  $W_0$  in this table.

$F_{\eta N}$	$\delta = 0$			$\delta = -7$			$\delta = -30$		
	$-V_0$	$-W_0$	$\sigma_{upp}$	$-V_0$	$-W_0$	$\sigma_{upp}$	$-V_0$	$-W_0$	$\sigma_{upp}$
CS [55]	97.7	21.9	6.5	72.5	10	6.88	44.3	2.7	-
M2 [63]	54.9	28.8	6.6	45.2	22	6.59	26.6	13	-
KSW [64]	68.4	32.6	6.57	56.8	22	6.67	38.7	13	6.5
IOV [65]	42.8	37.8	6.55	36.35	27.8	6.46	20.16	16.5	-
GW [54]	139	43.6	-	104	23.7	-	71.7	8.1	6.95

generalization of the optical potential [25] which can bring out interesting aspects related to the existence of the  $\eta$ -mesic helium. Hence, it is hoped that the optical model analysis of the present work should provide guidance in narrowing down the search for  $\eta$ -mesic  $^4\text{He}$ .

## Acknowledgements

We acknowledge the support from the Polish National Science Center through grant No. 2016/23/B/ST2/00784 and the Faculty of Science, Universidad de los Andes, Colombia, through project number P17.160322.007/01-FISI02. This work was partly supported by JSPS KAKENHI Grant Numbers JP16K05355 (S.H.) and JP17K05443 (H.N.) in Japan.

## References

- [1] P. Adlarson, et al., Search for  $\eta$ -mesic  $^4\text{He}$  in the  $dd \rightarrow ^3\text{He}n\pi^0$  and  $dd \rightarrow ^3\text{He}p\pi^-$  reactions with the WASA-at-COSY facility, Nucl. Phys. A 959 (2017) 102–115, <https://doi.org/10.1016/j.nuclphysa.2017.01.001>.
- [2] P. Adlarson, et al., Search for  $\eta$ -mesic  $^4\text{He}$  with the WASA-at-COSY detector, Phys. Rev. C 87 (3) (2013) 035204, <https://doi.org/10.1103/PhysRevC.87.035204>.
- [3] Y.K. Tanaka, et al., Measurement of excitation spectra in the  $^{12}\text{C}(p, d)$  reaction near the  $\eta'$  emission threshold, Phys. Rev. Lett. 117 (2016) 202501, <https://doi.org/10.1103/PhysRevLett.117.202501>.
- [4] H. Machner, Search for quasi bound  $\eta$  mesons, J. Phys. G 42 (2015) 043001, <https://doi.org/10.1088/0954-3899/42/4/043001>.
- [5] V. Metag, M. Nanova, E.Y. Paryev, Meson-nucleus potentials and the search for meson-nucleus bound states, Prog. Part. Nucl. Phys. 97 (2017) 199–216, <https://doi.org/10.1016/j.ppnp.2017.08.002>.
- [6] N. Ikeno, H. Nagahiro, D. Jido, S. Hirenzaki,  $\eta$ -nucleus interaction from the  $d + d$  reaction around the  $\eta$  production threshold, Eur. Phys. J. A 53 (2017) 194, <https://doi.org/10.1140/epja/i2017-12381-7>.
- [7] J.J. Xie, et al., Determination of the  $\eta^3\text{He}$  threshold structure from the low energy  $pd \rightarrow \eta^3\text{He}$  reaction, Phys. Rev. C 95 (1) (2017) 015202, <https://doi.org/10.1103/PhysRevC.95.015202>.
- [8] A. Fix, et al., Solution of the five-body  $\eta^4\text{He}$  problem with separable pole expansion method, Phys. Lett. B 772 (2017) 663–668, <https://doi.org/10.1016/j.physletb.2017.07.034>.
- [9] N. Barnea, B. Bazak, E. Friedman, A. Gal, Onset of  $\eta$ -nuclear binding in a pionless EFT approach, Phys. Lett. B 771 (2017) 297–302, <https://doi.org/10.1016/j.physletb.2017.05.066>.
- [10] N. Barnea, E. Friedman, A. Gal, Onset of  $\eta$ -meson binding in the He isotopes, Nucl. Phys. A 968 (2017) 35–47, <https://doi.org/10.1016/j.nuclphysa.2017.07.021>.
- [11] N. Barnea, E. Friedman, A. Gal, Few-body calculations of  $\eta$ -nuclear quasibound states, Phys. Lett. B 747 (2015) 345–350, <https://doi.org/10.1016/j.physletb.2015.06.010>.
- [12] E. Friedman, A. Gal, J. Mares, Eta-nuclear bound states revisited, Phys. Lett. B 725 (2013) 334–338, <https://doi.org/10.1016/j.physletb.2013.07.035>.
- [13] N.G. Kelkar, Momentum distribution of  $N^*$  in nuclei, Eur. Phys. J. A 52 (10) (2016) 309, <https://doi.org/10.1140/epja/i2016-16309-5>.
- [14] N.G. Kelkar, K.P. Khemchandani, N.J. Upadhyay, B.K. Jain, Interaction of eta mesons with nuclei, Rep. Prog. Phys. 76 (2013) 066301, <https://doi.org/10.1088/0034-4885/76/6/066301>.
- [15] N.G. Kelkar, Unresolved issues in the search for eta-mesic nuclei, Acta Phys. Pol. B 46 (1) (2015) 113–120, <https://doi.org/10.5506/APhysPolB.46.113>.
- [16] C. Wilkin, An introduction to mesic nuclei, Acta Phys. Pol. B 47 (2016) 249–260, <https://doi.org/10.5506/APhysPolB.47.249>.
- [17] C. Wilkin, Is there an  $\eta$  He-3 quasi-bound state?, Phys. Lett. B 654 (2007) 92–96, <https://doi.org/10.1016/j.physletb.2007.08.041>.
- [18] S.D. Bass, A.W. Thomas,  $\eta$  bound states in nuclei: a probe of flavor-singlet dynamics, Phys. Lett. B 634 (2006) 368–373, <https://doi.org/10.1016/j.physletb.2006.01.071>.
- [19] S.D. Bass, A.W. Thomas,  $\eta$ - $\eta'$  mixing in  $\eta$  mesic nuclei, Acta Phys. Pol. B 41 (2010) 2239–2247.
- [20] S. Hirenzaki, H. Nagahiro, Meson properties at finite density from mesic atoms and mesic nuclei, Acta Phys. Pol. B 45 (2014) 619–625, <https://doi.org/10.5506/APhysPolB.45.619>.
- [21] H. Nagahiro, D. Jido, S. Hirenzaki, Formation of eta-mesic nuclei by  $(\pi, n)$  reaction and  $N^*(1535)$  in medium, Phys. Rev. C 80 (2009) 025205, <https://doi.org/10.1103/PhysRevC.80.025205>.
- [22] H. Nagahiro, et al., Formation of  $\eta(958)$ -mesic nuclei by  $(p, d)$  reaction, Phys. Rev. C 87 (4) (2013) 045201, <https://doi.org/10.1103/PhysRevC.87.045201>.
- [23] S. Hirenzaki, et al., Formation of  $\eta$ -mesic nuclei, Acta Phys. Pol. B 41 (2010) 2211–2220.
- [24] S. Wycech, W. Krzemien, Studies of mesic nuclei via decay reactions, Acta Phys. Pol. B 45 (3) (2014) 745–751, <https://doi.org/10.5506/APhysPolB.45.745>.
- [25] J. Niskanen,  $\eta$ -nuclear interaction: optical model versus coupled-channels approach, Phys. Rev. C 92 (5) (2015) 055205, <https://doi.org/10.1103/PhysRevC.92.055205>.
- [26] Q. Haider, L.C. Liu, Formation of an mesic nucleus, Phys. Lett. B 172 (1986) 257–260, [https://doi.org/10.1016/0370-2693\(86\)90846-4](https://doi.org/10.1016/0370-2693(86)90846-4).
- [27] R.S. Bhalerao, L.C. Liu, Off-shell model for threshold pionic eta production on a nucleon and for  $\eta n$  scattering, Phys. Rev. Lett. 54 (1985) 865–868, <https://doi.org/10.1103/PhysRevLett.54.865>.
- [28] A.M. Green, J.A. Niskanen, S. Wycech, Eta-deuteron scattering, Phys. Rev. C 54 (1996) 1970, <https://doi.org/10.1103/PhysRevC.54.1970>.
- [29] C. Wilkin, Near-threshold production of  $\eta$  mesons, Phys. Rev. C 47 (1993) 938, <https://doi.org/10.1103/PhysRevC.47.938>.
- [30] S. Wycech, A.M. Green, J.A. Niskanen, Are there eta helium bound states?, Phys. Rev. C 52 (1995) 544, <https://doi.org/10.1103/PhysRevC.52.544>.
- [31] J. Berger, et al., Identification of the  $d + p \rightarrow ^3\text{He}n$  reaction very near threshold: cross section and deuteron tensor analyzing power, Phys. Rev. Lett. 61 (1988) 919–922, <https://doi.org/10.1103/PhysRevLett.61.919>.
- [32] B. Mayer, et al., The reactions  $pd \rightarrow ^3\text{He}n$  and  $d + p \rightarrow ^3\text{He}n + \pi^-$  near the eta threshold, Phys. Rev. C 53 (1996) 2068–2074, <https://doi.org/10.1103/PhysRevC.53.2068>.
- [33] G.A. Sokol, L.N. Pavlyuchenko, arXiv:nucl-ex/0111020.
- [34] J. Smysrski, et al., Measurement of the  $dp \rightarrow ^3\text{He}n$  reaction near threshold, Phys. Lett. B 649 (2007) 258–262, <https://doi.org/10.1016/j.physletb.2007.04.021>.
- [35] T. Mersmann, et al., Precision study of the eta He-3 system using the  $dp \rightarrow ^3\text{He}n$  reaction, Phys. Rev. Lett. 98 (2007) 242301, <https://doi.org/10.1103/PhysRevLett.98.242301>.
- [36] A. Budzanowski, et al., Search for  $\eta$ -mesic nuclei in a recoil-free transfer reaction, Phys. Rev. C 79 (2009) 012201, <https://doi.org/10.1103/PhysRevC.79.012201>.
- [37] M. Papenbrock, et al., Absence of spin dependence in the final state interaction of the  $\bar{d}p \rightarrow ^3\text{He}n$  reaction, Phys. Lett. B 734 (2014) 333, <https://doi.org/10.1016/j.physletb.2014.05.079>.
- [38] P. Moskal, J. Smysrski, Acta Phys. Pol. B 41 (2010) 2281–2292.
- [39] Q. Haider, L.C. Liu, Interference and nuclear medium effects on the eta-mesic nuclear spectrum, J. Phys. G 37 (2010) 125104, <https://doi.org/10.1088/0954-3899/37/12/125104>.
- [40] B. Krusche, C. Wilkin, Production of  $\eta$  and  $\eta'$  mesons on nucleons and nuclei, Prog. Part. Nucl. Phys. 80 (2014) 43–95, <https://doi.org/10.1016/j.ppnp.2014.10.001>.
- [41] P. Moskal, Few-body aspects of the near threshold pseudoscalar meson production, Few-Body Syst. 55 (2014) 667–674, <https://doi.org/10.1007/s00601-014-0854-y>.
- [42] M. Skurzok, et al., Upper limits for the production of the  $\eta$ -mesic helium in the  $dd \rightarrow ^3\text{He}n\pi^0$  and  $dd \rightarrow ^3\text{He}p\pi^-$  reactions, Acta Phys. Pol. B 47 (2016) 503–508, <https://doi.org/10.5506/APhysPolB.47.503>.
- [43] P. Moskal, Search for exotic hadronic matter: tetraquarks, pentaquarks, dibaryons and mesic nuclei, Acta Phys. Pol. B 47 (2016) 97–108, <https://doi.org/10.5506/APhysPolB.47.97>.
- [44] P. Moskal, M. Skurzok, W. Krzemien, Status and perspectives of the search for eta-mesic nuclei, AIP Conf. Proc. 1753 (2016) 030012, <https://doi.org/10.1063/1.4955353>.
- [45] C. Wilkin, The legacy of the experimental hadron physics programme at cosy, Eur. Phys. J. A 53 (6) (2017) 114–302, <https://doi.org/10.1140/epja/i2017-12295-4>.
- [46] J. Kulpa, S. Wycech, The absorptive  $\rho^2$  terms in the  $\eta$  optical potential, Acta Phys. Pol. B 29 (1998) 3077.
- [47] S. Wycech, W. Krzemien, Studies of mesic nuclei via decay reactions, Acta Phys. Pol. B 45 (2014) 745, <https://doi.org/10.5506/APhysPolB.45.745>.
- [48] R. Frascaia, et al., Total  $dd \rightarrow \alpha + \eta$  cross sections near threshold, Phys. Rev. C 50 (2) (1994) R537–R540, <https://doi.org/10.1103/PhysRevC.50.R537>.
- [49] N. Willis, et al., Eta-helium quasibound states, Phys. Lett. B 406 (1997) 14–19, [https://doi.org/10.1016/S0370-2693\(97\)00650-3](https://doi.org/10.1016/S0370-2693(97)00650-3).
- [50] A. Wrońska, et al., Near threshold eta meson production in the  $dd \rightarrow ^4\text{He} + \eta$  reaction, Eur. Phys. J. A 26 (2005) 421–428, <https://doi.org/10.1140/epja/i2005-10185-0>.
- [51] P. Moskal, et al., Eta-prime production in proton proton scattering close to threshold, Phys. Rev. Lett. 80 (1998) 3202–3205, <https://doi.org/10.1103/PhysRevLett.80.3202>.
- [52] A. Nogga, Ruhr Universität Bochum, Ph.D. Thesis.
- [53] M. Skurzok, Jagiellonian University, Ph.D. Thesis.
- [54] A.M. Green, S. Wycech,  $\eta$ -nucleon scattering length and effective range uncertainties, Phys. Rev. C 71 (2005) 014001, <https://doi.org/10.1103/PhysRevC.71.014001>.
- [55] A. Cieplý, J. Smejkal, Chirally motivated separable potential model for  $\eta n$  amplitudes, Nucl. Phys. A 919 (2013) 46, <https://doi.org/10.1016/j.nuclphysa.2013.10.003>.

- [56] E.Z. Liverts, N. Barnea, Transition states and the critical parameters of central potentials, *J. Phys. A* 44 (2011) 375303, <https://doi.org/10.1088/1751-8113/44/37/375303>.
- [57] A. Deloff, Product representation in effective range theory, *Nucl. Phys. A* 303 (1978) 412.
- [58] M. Arndt, et al., Observation of a zero-energy resonance in Cs–Cs collisions, *Phys. Rev. Lett.* 79 (1997) 625, <https://doi.org/10.1103/PhysRevLett.79.625>.
- [59] A. Cieplý, E. Friedman, A. Gal, J. Mareš, In-medium  $\eta N$  interactions and  $\eta$  nuclear bound states, *Nucl. Phys. A* 925 (2014) 126, <https://doi.org/10.1016/j.nuclphysa.2014.02.007>.
- [60] N. Barnea, et al., Onset of  $\eta$  nuclear binding, [arXiv:1712.05643](https://arxiv.org/abs/1712.05643).
- [61] Q. Haider, L.C. Liu, Eta-mesic nuclei: past, present, future, *Int. J. Mod. Phys. E* 24 (2015) 1530009, <https://doi.org/10.1142/S021830131530009X>.
- [62] T. Hoshino, et al., Constraining the  $\bar{K}N$  interaction from the 1s level shift of kaonic deuterium, *Phys. Rev. C* 96 (2017) 045204, <https://doi.org/10.1103/PhysRevC.96.045204>.
- [63] M. Mai, P.C. Bruns, U.-G. Meissner, Pion photoproduction off the proton in a gauge-invariant chiral unitary framework, *Phys. Rev. D* 86 (2012) 094033.
- [64] N. Kaiser, P.B. Siegel, W. Weise, Chiral dynamics and the  $S_{11}(1535)$  nucleon resonance, *Phys. Lett. B* 362 (1995) 23, [https://doi.org/10.1016/0370-2693\(95\)01203-3](https://doi.org/10.1016/0370-2693(95)01203-3).
- [65] T. Inoue, E. Oset, J.V. Vacas, Chiral unitary approach to s-wave meson baryon scattering in the strangeness  $s = 0$  sector, *Phys. Rev. C* 65 (2002) 035204, <https://doi.org/10.1103/PhysRevC.65.035204>.
- [66] S.A. Rakityansky, et al., Quasibound states of  $\eta$ -nucleus systems, *Phys. Rev. C* 53 (1996) R2043, <https://doi.org/10.1103/PhysRevC.53.R2043>.
- [67] N.G. Kelkar, Quantum reflection and dwell times of metastable states, *Phys. Rev. Lett.* 99 (2007) 210403, <https://doi.org/10.1103/PhysRevLett.99.210403>.